Filters for HST Wide Field Camera 3

S. Baggett[*a], T. Brown[a], R. Boucarut[b], D. Figer[a], G. Hartig[a], R. Kimble[b], J. MacKenty[a], M. Robberto[a], R. Telfer[c], J. Kim-Quijano[a], M. Quijada[b], G. Allen[d], P. Arsenovic[b], B. Hilbert[a], O. Lupie[b], J. Townsend[b]

[a] Space Telescope Science Institute, 3700 San Martin Dr, Baltimore, MD 21218
[b] NASA/Goddard Space Flight Center, Greenbelt, MD 20771
[c] Orbital Sciences Corporation, Beltsville, MD 20705
[d] Barr Associates, Inc., 2 Lyberty Way, Westford, MA 01886

ABSTRACT

Wide-Field Camera 3 (WFC3) has been built for installation on the Hubble Space Telescope (HST) during the next servicing mission. The WFC3 instrument consists of both a UVIS and an IR channel, each with its own complement of filters. On the UVIS side, a selectable optical filter assembly (SOFA) contains a set of 12 wheels that house 48 elements (42 full-frame filters, 5 quadrant filters, and 1 UV grism). The IR channel has one filter wheel which houses 17 elements (15 filters and 2 grisms). While the majority of UVIS filters exhibited excellent performance during ground testing, a subset of filters showed filter ghosting; improved replacements for these filters have been procured and installed. No filter ghosting was found in any of the IR filters; however, the new IR detector for WFC3 will have significantly more response blueward of 800 nm than the original detector, requiring that two filters originally constructed on a fused silica substrate be remade to block any visible light transmission. This paper summarizes the characterization of the final complement of the WFC3 UVIS and IR filters, highlighting improvements in the replacement filters and the projected benefit to science observations.

Keywords: Hubble Space Telescope, visible, UV, infrared, filter characterization, filter ghosts

1. INTRODUCTION

WFC3 has been developed as a panchromatic camera with two channels covering the UVIS (200-1000 nm) and IR (0.8-1.7 μm) ranges. The relatively wide field of view (160”x160”) in the UVIS channel is imaged with a 4Kx4K E2V CCD detector; the IR field of view (123”x139”) is imaged with a 1Kx1K Rockwell focal plane array. Designed to fully cover the wavelength regions using a mix of bandwidths, the filter sets to be used in these channels were originally chosen based upon community input, the WFC3 Science White Paper (Stiavelli & O’Connell), a suite of WFC3 Science Oversight Committee (SOC)-developed test proposals representing current astronomical studies, and statistics of historical filter use in other HST instruments. With these recommendations, the WFC3 IPT (Integrated Product Team) developed detailed requirements for each filter for the vendors who designed and manufactured the filters; the final elements were characterized, evaluated, and installed into the filter wheels.

During instrument-level ground testing in 2003-2004, most of the WFC3 UVIS filters performed very well, consistent with or exceeding expectations. A number of filters, however, were found to have filter ghosts; the problems were traced to the filter designs used, such as air-gap (two substrates joined via thin spacers) or multi-substrate (a stack of two or more substrates bonded or laminated together with a layer of optical adhesive). Air-gaps were employed as a last resort during the design and manufacture of the original filters (~2000-2002) because the adhesive in multi-substrate filters significantly reduced the throughput in UV filters and introduced substantial non-uniformity in visible narrow band filters. The multi-substrate laminated designs were used at that time in the medium and wide band visible filters as they were easier and more straightforward to produce than equivalent single substrate filters. However, if the reflective

[*] email sbaggett@stsci.edu; phone 410-338-5054

Space Telescopes and Instrumentation I: Optical, Infrared, and Millimeter,
edited by John C. Mather, Howard A. MacEwen, Mattheus W.M. de Graauw,
Proc. of SPIE Vol. 6265, 626532, (2006) · 0277-786X/06/$15 · doi: 10.1117/12.672300

coatings deviate slightly from the design models, particularly in the wings of the bandpass (where the ratio of reflected to in-band light is large), the result can be filter ghosting.

Figure 1 shows examples of typical air-gap and multi-substrate filter ghosts (Brown & Lupie, 2003). As can be seen from the images, air-gap ghosts appear as extended, elaborately shaped features that vary dramatically as the PSF is moved across the field of view; ground testing (instrument level thermal vacuum tests as well as later laboratory tests on filters alone) revealed that the ghost strengths vary strongly with wavelength as well. The ghost strengths typically peak well outside of the filter bandpass; of course, a higher ratio of ghost to primary image can be tolerated at wavelengths where the filter transmission is low. Ghosts in multi-substrate laminated filters tend to be more point-like as the offending reflections arise from surfaces less widely spaced than in air-gap filters. These multi-substrate ghosts show only slight variations as a function of PSF position within the field of view but do vary strongly as a function of wavelength, typically peaking at the edges of the filter bandpass.

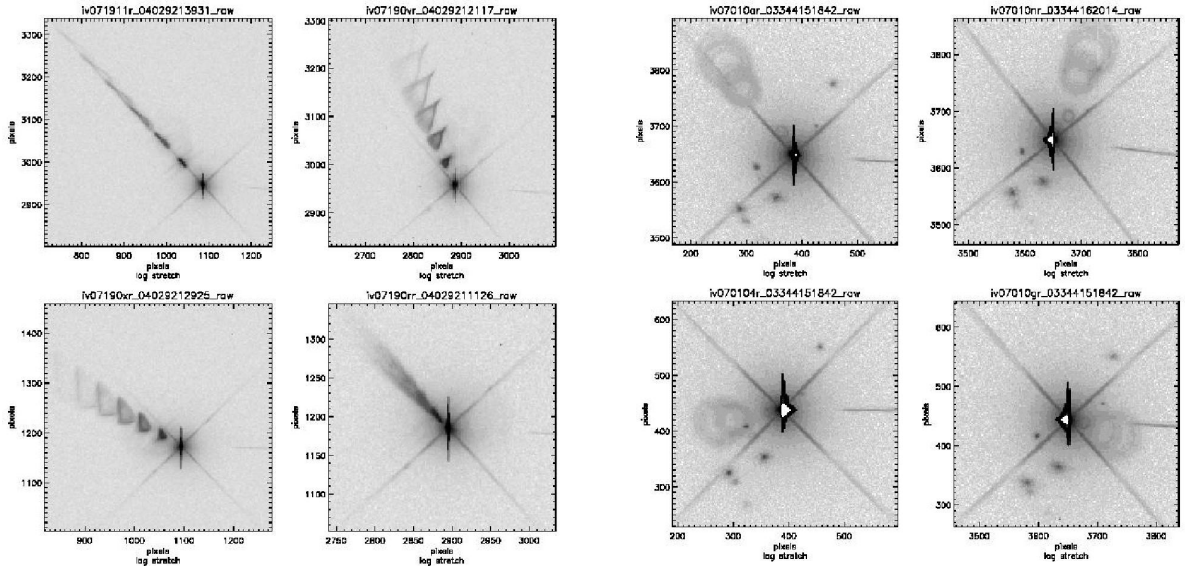

Fig 1. The four images at left and at right illustrate air-gap and multi-substrate ghost behavior, respectively (from Brown & Lupie, 2003; F225W and F606W filters). The image greyscale has been inverted to highlight the ghosts. Each set of four show image subsections centered in the four quadrants of the WFC3 field of view, taken with white (xenon lamp) light during instrument level ground testing. The horizontal linear feature to the right of the PSF is a test setup artifact. The large ring-like ghosts in the multi-substrate images on the right had been predicted and are due to reflections in the CCD windows; though readily apparent in these highly stretched images of saturated sources, the fraction of the target light per pixel in the window ghosts is low.

The strongest ghosts were found in the UV filters such as F225W (bandpass ~200-290 nm), where filter ghosts measured in white light comprised a total of 15% of the PSF light, and F218W (bandpass ~190-250 nm) and F280N (~277-283 nm), each with ~10% total in ghosts; most of the remaining affected filters each had ghosts totaling 1% or less. Obviously, ghosts are undesirable and would visually degrade any image; however, the scientific impact of the WFC3 filter ghosts was shown to depend upon the specific target type (Bond & Brown, 2005). Stellar photometry of star clusters, for example, appears to be the least affected: color magnitude analysis performed on simulated ghost-free and ghost-affected images show that while the images with ghosts are visually unappealing, most of the photometry is retrievable with just some small additional scatter in the results. In addition, the effects of ghosts in small fields with simply-shaped targets might be sufficiently correctable (e.g., with deconvolution techniques) to allow morphological studies and/or rudimentary measurements such as total brightness (Bond & Brown, 2005). However, deconvolving more extended fields becomes difficult if not impossible because the WFC3 PSF varies considerably across the field of

view. Workarounds such as dithering (applying slight pointing offsets between images) or rolling the telescope (rolling the field of view) between observations might allow for some correction of the ghosts but these techniques would necessitate more observing time, place more restrictions on scheduling science programs, and require significantly more calibration effort on the part of the observer after the images are acquired. As Bond & Brown (2005) point out, these techniques would fail to work for crowded or extended targets, effectively limiting WFC3's ability to provide scientifically useful images with the most severely affected filters in the original WFC3 complement.

Given the projected negative impact to WFC3 science combined with the availability of additional instrument development time due to the delay in the HST servicing mission to install WFC3, the decision was taken to procure new replacement filters for the worst offenders. Furthermore, a lab setup (discussed in next section) producing a WFC3-like beam was developed to enable direct imaging checks of the filters as part of the characterization tests, to be completed and assessed before the elements are installed into a filter wheel. Based upon lessons-learned with WFC3, *the authors highly recommend other missions employing imaging filters model the strength of inter-surface ghost reflections at the filter design stage and include acceptance tests of the filters in an optical configuration similar to how they will be used in the final instrument*.

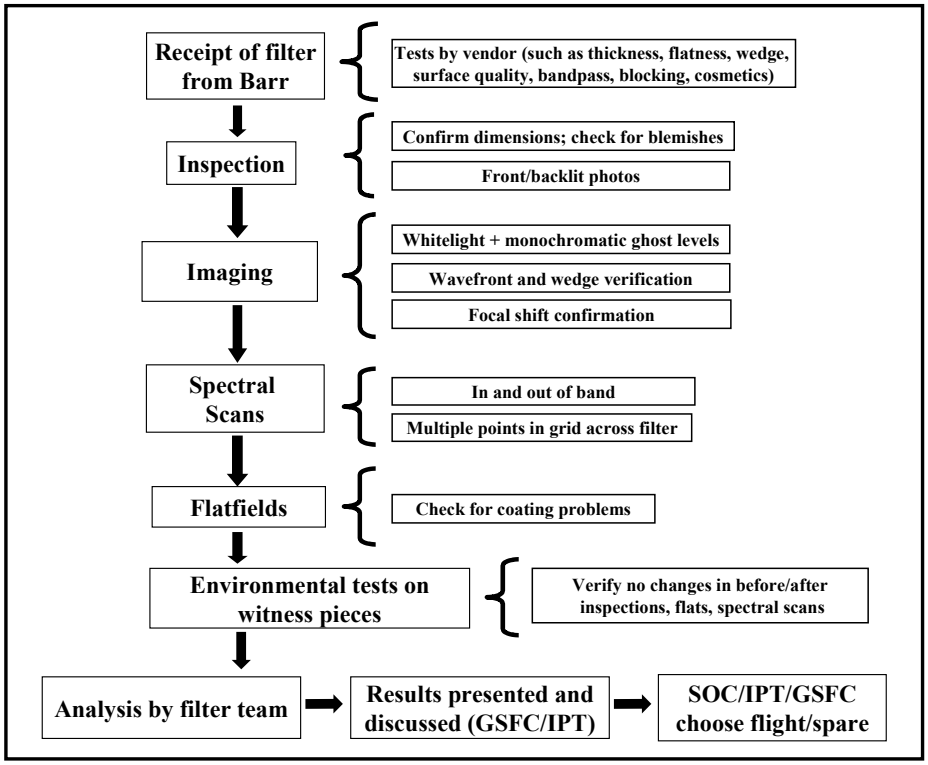

Fig 2. Summary of characterization test procedure.

In the years since the construction of the original WFC3 filter set, the manufacturing process had matured such that reasonable throughputs and uniformity can now be obtained using single substrate designs; along with judicious placement of coatings, the ghosting problem can be substantially reduced. Single-substrate replacements for the affected filters have been successfully procured and subjected to a rigorous set of characterization tests designed to verify conformance of the new filters to the filter requirements. The tests performed are based upon the test suite used for the first generation filters (Raouf & Trauger, 2003) and expanded to include a variety of imaging checks as well. The characterization process is summarized in Figure 2. It begins at the vendor, where numerous verification steps are

performed during manufacturing and before shipment of the filters to GSFC. Upon receipt at GSFC, the filters undergo further extensive testing, including a detailed visual inspection, imaging tests (point source and flatfield), spectral scans, and environmental checks. Results are analyzed in light of the filter specifications (JPL D18189; CEI STE-66) and discussed within the WFC3 team; recommendations for potential replacement filters are presented to the WFC3 Science Oversight Committee (SOC) for their evaluation. The WFC3 SOC determines the final choice of flight/spare filters.

In the IR channel, no filter ghosts were found during instrument-level testing, but two filters originally constructed on fused silica - because the original IR detector was illuminated through a CdZnTe substrate that provided a strong blue cutoff - have been remade on Hoya IR80, an IR-transmitting colored glass. The new IR detector under development is driving the change: the CdZnTe substrate is being removed to reduce particle-induced luminescence seen in the original detector; however, this significantly increases the QE blueward of 800 nm. In addition to the two IR filters being remade, the two IR grisms have been removed to correct an installation problem; they will be reinstalled in the upcoming year. One of the grisms, because it was being removed anyway, was remade with an improved red edge in order to reduce the transmission of thermal background radiation that led to an undesirably high background on the detector during thermal vacuum testing. The IR replacement filters and grism underwent a full set of characterization tests similar to the UVIS filter replacements, based upon the test suite performed on the original IR filters (Boucarut et al., 2001; TM028642) and expanded to include direct imaging checks.

The following sections summarize the UVIS and IR replacement filter characterization tests and provide an overview of the resulting final WFC3 filter sets.

2. CHARACTERIZATION TESTS

Vendor Tests
The manufacturer performs comprehensive checks during production and prior to shipment of the filter to the customer. These tests verify the filters' compliance with the requirements and the robustness of the filter coating. Key items measured on the candidate flight pieces include the spectral throughput (primary bandpass as well as out-of-band blocking), transmissive wavefront (on the uncoated substrate as well as the coated filter), and quality control (check of length, width, thickness, inspection for scratches and cosmetic defects, painting of any pinholes, and cleaning). Characteristics such as the coating integrity (adhesion quality, resistance to abrasions, temperature and humidity cycling) and radiation hardness are performed on witness or flight-like pieces. Final pieces are inspected and shipped to GSFC for further testing.

UVIS Imaging Tests
Once the filters have arrived at GSFC and undergone an incoming inspection, imaging tests are performed using FilterGEISt (Filter Ghost Evaluation Imaging Station). The FilterGEISt is a dedicated lab setup developed specifically to test the WFC3 replacement filters. It reproduces the WFC3 UVIS + HST optical parameters (f/31 beam). A key component is a 4-axis stage assembly that provides repeatable translation and tip/tilt motions as well as simulations of positions within the WFC3 FOV. Images are acquired with an SBIG ST6 CCD camera mounted on a motorized translation stage for focus adjustments. M.Quijada et al., this conference provides further FilterGEISt details.

Extensive point source imaging is done with each filter, using white (either xenon or deuterium lamp) as well as monochromatic (200-1000 nm) light. These data allow for measurement of filter ghosts (strength, appearance, and spatial behavior), as well as for verification of wavefront, wedge, and focus shift. A typical white light image taken through a filter is shown in Figure 3a. For ghost measurements, images are obtained at a variety of filter tilt angles and translation positions as well as in configurations simulating seventeen points distributed across the WFC3 field of view. The specification calls for less than 0.2% of the total incident (white) light to fall within a discrete ghost image (STE-66). Point source images are also taken at a full set of monochromatic wavelengths, typically 200-1000 nm in steps of 10 nm, with 8 nm bandpass shortward, and 16 nm bandpass longward, of 550 nm. Measurements from a typical monochromatic scan are shown in Figure 3b along with a filter model based upon theoretical transmission curves of the various filter coatings. Ghost levels as a function of wavelength are used to verify coating behavior and constrain the model, which in turn is used to predict ghost behavior as a function of spectral type for astronomical sources.

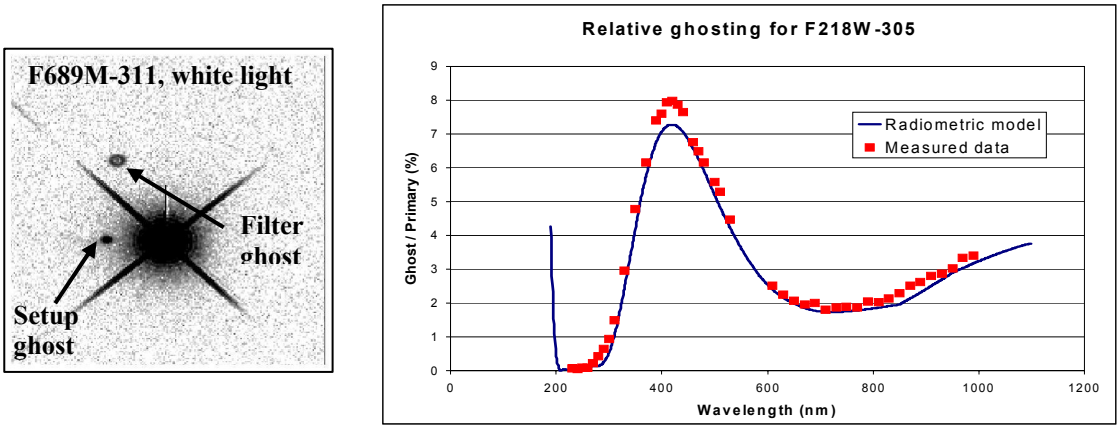

Fig 3. a) At left is a typical white light point source image, shown with an inverted greyscale, taken through a candidate replacement filter. To facilitate measurements of the ghost level (in this case, <0.1%), the ghost has been moved away from the PSF by using a relatively high filter tilt angle in the lab setup. The ghost marked "setup" to the left of the PSF is not filter-related but due to the CCD window of the camera used in the lab setup. b) The plot at right shows monochromatic ghost levels measured as a function of wavelength (squares) and the filter model (solid line); the fit is very good. Note that for the filter shown (F218W, bandpass ~190-250 nm) the relatively high ghost levels peak at ~420 nm, well out-of-band, where the filter blocking is significant: integrated over a continuum source the relative ghost strengths are much lower.

FilterGEISt is also used to obtain a series of defocused images, or focus sweeps (see Figure 4), in a 9x9 grid of 11 mm diameter beam covering the filter, separated by steps of 5 mm. Reference focus sweeps taken without a filter are subtracted, and phase retrieval analysis, including focus and tilt, yields the wavefront error, focus shift, and wedge. The wavefront accuracy at 633 nm is required to be 1/30 and 1/15 wave (single substrate and multi-substrate filters, respectively) peak to valley over a 10 mm diameter circle (JPL drawing 1019572). The specification for the UVIS filters (JPL D18189; STE-66) requires the focus shift at 633 nm of each filter to be the equivalent of a 5.5 ± 0.1 mm thick plano/plano fused silica substrate plus the shift of two fused silica CCD windows (8.382 and 2.540 mm thick). This ensures that the filters will be parfocal, i.e., the focus will not change as filters are changed. The allowable wedge, the angle between the two outer surfaces of each filter, must be less than 0.01524 mm across the 57.3 mm aperture, in order to result in no more than a 0.5 detector pixel relative displacement (STE-66). Based upon the resulting median direction and magnitude of PSF displacement seen in the phase retrieval data, the filters are mounted into the filter wheel with an orientation minimizing relative displacements between filters.

In addition to point source imaging, the FilterGEISt can be reconfigured to take flatfields, simulating the WFC3 internal calibration flatfield system (divergent beam). An array of 11x11 images is taken to completely cover a filter; individual pixels in an image cover about 17x20 μm on the filter. Flatfields are obtained with either the xenon or deuterium lamp, depending upon the filter (the xenon spectrum is relatively red so UV filters are typically done with the deuterium lamp). The resulting flatfields provide a detailed map of the fine scale transmission properties of the filter and are checked for blemishes, pinholes, coating degradation, or any other anomalies that may be present. For example, scattered light seen in a corner of one flatfield was found to be due to an unpainted pinhole near the edge of the filter; painting the pinhole reduced the scattering significantly.

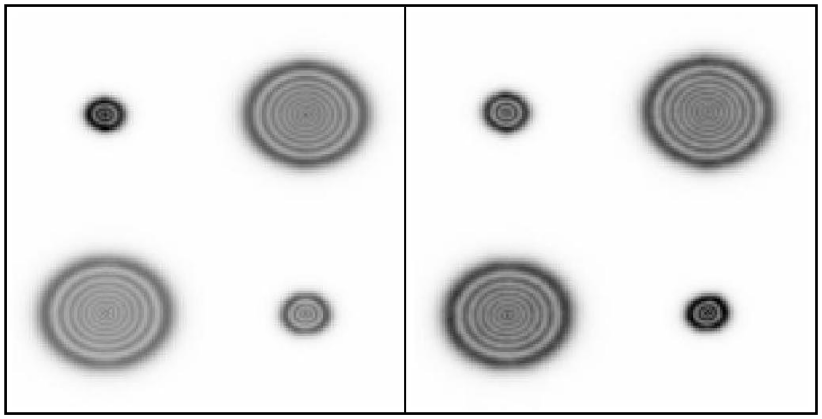

Fig. 4. Examples of typical phase retrieval images. Both are at 606 nm; at left are images taken without a filter, at right are images taken through a candidate F606W.

Spectral Scans (UVIS)

The spectral throughput of a filter is measured both in and out-of-band using a PerkinElmer 950 high performance grating spectrophotometer. UVIS filters are square, 57.3 mm on a side; the clear aperture and coated clear aperture are 53.238 mm and 55.27 mm, respectively. To assess uniformity, in-band UVIS scans are performed in a 5x5 grid across the filters, while out-of-band UVIS scans are executed in the center of the filter and at the four corners. Figure 5 illustrates typical in and out-of-band scans; the data are used to derive measurements of critical parameters (such as peak and average transmittance, central wavelength, bandpass shape, depth of ripples, and out-of-band rejection) that are evaluated in light of the input specifications (JPL D18189).

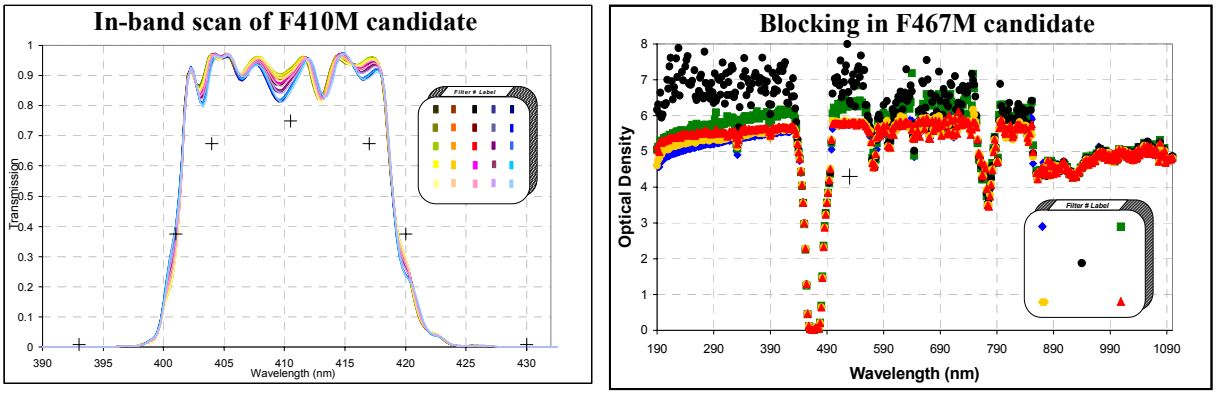

Fig. 5. Examples of in and out-of-band scans (left and right plot, respectively) for candidate UVIS filters. Transmission of the in-band data is plotted as a function of wavelength; out-of-band plot presents optical density (OD = $-\log_{10}(T)$) as a function of wavelength. Locations of the scan on the filter are noted in the accompanying diagram; some of the specifications for the filter are marked with '+' symbol. While the majority of dips in the out-of-band OD are real, the overall drop in the out-of-band OD level around 870 nm is artificial: the spectrophotometer switches detectors in that region, resulting in a change in sensitivity. The actual OD redward of 870 nm is better by at least ~1 (for more details, see discussion in Quijada et al., this conference).

Environmental Tests

In addition to the tests performed by the vendor, filter witnesses and non-flight pieces are subjected to temperature cycling under thermal vacuum (TV) conditions in order to verify the robustness of the coatings. Baseline inspections, spectral scans, and flatfields are taken prior to thermal cycling. The test is designed to mimic the thermal vacuum conditions the filters are expected to experience during storage and ground testing (-20°C to +40°C, <40% relative humidity (RH)) and on-orbit operations (0 ± 5 °C, survival range -20°C to +40°C, <40% RH, $<10^{-6}$ Torr pressure). After the cycles, another round of inspections, spectral scans, and flatfields are taken and compared to the pre-cycling data to check for any evidence of coating degradation such as delamination or crazing.

IR Filter Testing

The characterization test suite for the IR filters is similar to that for the UVIS filters. The FilterGEISt can be converted to simulate the IR channel (f/11 beam); an IR InGaAs IR array camera (40 μm pixels) acquires the images. The resulting IR data are used to perform ghost checks as well as to measure wavefront, focus shift, and wedge. Point source imaging is done at a variety of rotation and translation points, but because the filters are relatively small (25.4 ± 0.1 mm diameter round, 22 mm clear aperture), fewer points are used to cover the filter. As with the original IR flight filters, no white light filter ghosts were detected; no monochromatic imaging was performed.

Focus sweeps were obtained in a 3x3 array of positions across the filter, using an 11 mm beam diameter and 8 nm bandpass. As for the UVIS filters, reference focus sweeps taken without a filter are subtracted; phase retrieval analysis, including focus and tilt, provides the wavefront error, focus shift, and wedge. The requirements for the IR filters (STE-66) stipulate that they not displace the image on the detector by more than 0.2 detector pixels or degrade the image quality by more than 0.02 waves (at 633 nm; transmitted wavefront over the full 22 mm diameter aperture must be less than 0.02 waves rms), which the new filters easily satisfy. To maintain parfocality, the filters must be the equivalent to 4.0 ± 0.1 mm of fused silica and the wedge angle must be less than 10 arcsec.

Spectral scans are done at several locations on the filter to monitor coating uniformity and at two temperatures (room temperature and nominal operating temperature of -30C). Given the relatively small filter size, the in-band IR scans are performed at 5 points and the out-of-band scans at filter center, as illustrated in Figure 6. The new filters possess nearly perfect bandpass shapes, very uniform across the filter; there were no significant variations with temperature.

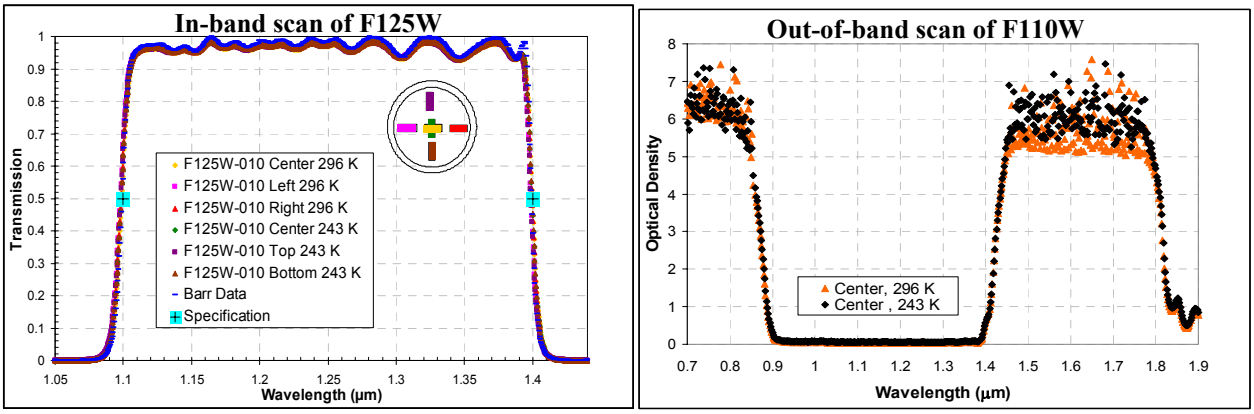

Fig. 6. Examples of in and out-of-band scans (left and right plot, respectively) for two IR filters. In-band scans are taken at three points each at room and operating temperatures.

3. FINAL FILTER SETS

UVIS

The final choice of which, if any, replacement filters to fly resides with the WFC3 Science Oversight Committee, with analysis inputs from the STScI and GSFC WFC3 teams. The decision is based upon a careful balance of the characterization test results for the new filters versus the characteristics of the original flight filters as determined from instrument-level ambient and thermal vacuum tests as well as the risk of replacing a filter. In all, a total of 11 UVIS filters have been replaced with improved versions satisfying or surpassing the requirements: 4 wide band UV and 2 wide band visible filters, 3 medium band visible filters, and two narrow bands (1 UV and 1 visible). In most cases, the filter manufacturing technology now available has not only reduced the ghost levels as desired and significantly simplified the ghost shape and behavior across the field of view (as expected for single substrate designs) but also provided increased throughput. For example, the original F225W filter (bandpass ~200-290 nm) exhibited the worst ghosting of all the original filters: about 15% of the total light in a PSF resided in filter ghosts. In the new F225W, the ghost levels are reduced to less than 0.3 percent and the filter grasp (integral of the filter and WFC3 transmission over wavelength in the primary bandpass) is about 30% higher than with the original flight filter. The one exception was F218W (bandpass 190-250 nm); in this case the ghost level was reduced and the shape/behavior simplified as intended but the throughput was reduced as well. Several runs were produced at the vendor but the throughputs remained consistently lower than in the original air-gap filter. However, even with the penalty of less grasp, the WFC3 team recommendation and SOC decision was to replace the filter because, in addition to the ghost issue, there was concern about the stability of the UV air-gap coatings: flatfields and photometric monitoring during instrument-level testing showed evidence of some slight time-dependent behavior. The cause of the variability was never definitively identified; however, given the importance of the F218W filter as the shortest wavelength WFC3 filter, the reduced ghost levels and proven coating stability in the new single-substrate F218W, the replacement was performed. Figure 7 (left) provides a comparison of the original and new UV filter bandpasses.

As in the UV, ghost levels in the new visible filters were reduced as well (some even eliminated) and again the grasps of the new filters are higher than in the old filters. Figure 7 (right) provides a comparison of the bandpasses of the original and new broad / medium band visible filters. The new medium band filters provide excellent performance; however, they also exhibit somewhat more ripple, or localized drops in throughput, across the top of the bandpass. The specification (JPL 18189D) states that ripples within the 90% passband should not fall below 90% of the peak transmission. The new single-substrate medium bands violate this requirement slightly but were deemed acceptable as replacements in light of 1) the excellent performance of the filters in all other areas and 2) the results of simulations which showed no noticeable difference in the recovery of spectral energy distributions when using one of the rippled bands versus a perfectly smooth-topped hypothetical filter (edges matching those of the new filters). Minor differences (~1% photometric effects as the test target was red and blueshifted ±800 km/sec against the filter bandpass) were found to be due not to any ripple but to spectral features moving across the bandpass edges.

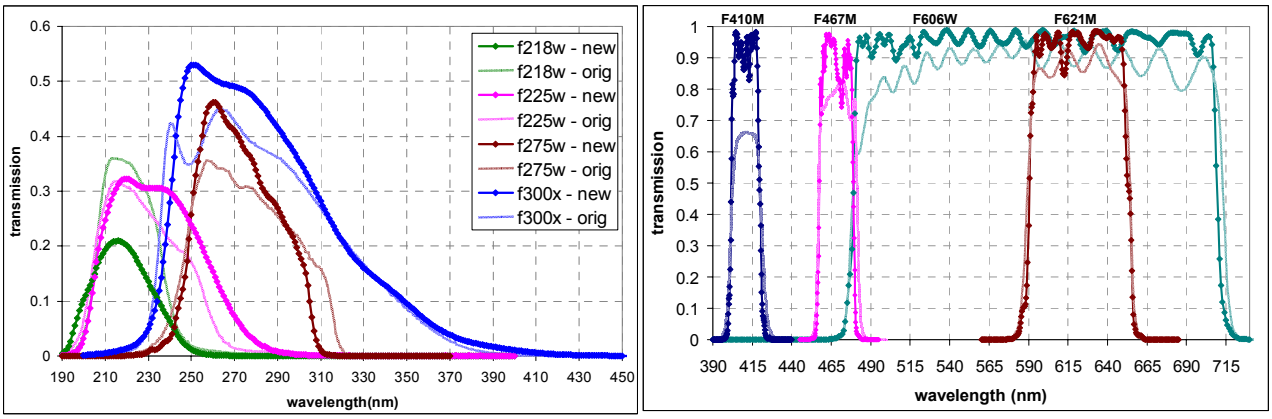

Fig. 7. Comparison of most of the replacement filters with the original versions; UV and visible filters are shown in the left and right plots, respectively. In both graphs, a given bandpass is shown in the same color, with the original filter in a light pattern and the new filter in a bold pattern.

The complete UVIS filter complement is shown in Figure 8; filter names generally reflect the central wavelength of the filter while the last letter in the name indicates bandwidth. As the figure illustrates, the WFC3 UVIS filter set consists of a small number of extremely wide long pass filters (e.g., F350LP and F600LP), a variety of wide as well as medium band filters, a large number of narrow band filters, and one UV grism (~220-400 nm). The filters reside in 12 wheels, four filters per wheel, housed in the SOFA (selectable optical filter assembly mechanism refurbished from the Wide Field Planetary Camera 1 which flew 1990-1993 on HST). The total number of UVIS filters shown in Figure 8 exceeds the number of available slots thanks to the development of "quad filters" – in these cases, the spectral element is partitioned into 4 quadrants, each containing a different bandpass (typically a narrow band). Each quadrant of course nominally covers only ¼ of the WFC3 total field of view or about 80"x80" (edge effects due to the size of the beam footprint will result in an unvignetted field somewhat smaller than the ¼ FOV). However, the use of the five quads on WFC3 has significantly increased the number of available narrow band filters, complementing HST's ACS (Advanced Camera for Surveys), which has relatively few narrow band filters (ACS does have "ramp" filters, where the bandpass changes relatively rapidly across the element but with a commensurate small field of view). The WFC3 narrow band filters will enable emission and absorption line studies of a large variety of targets, not only stars but protostars/planetary disks, planetary nebulae, supernova remnants, and the interstellar medium.

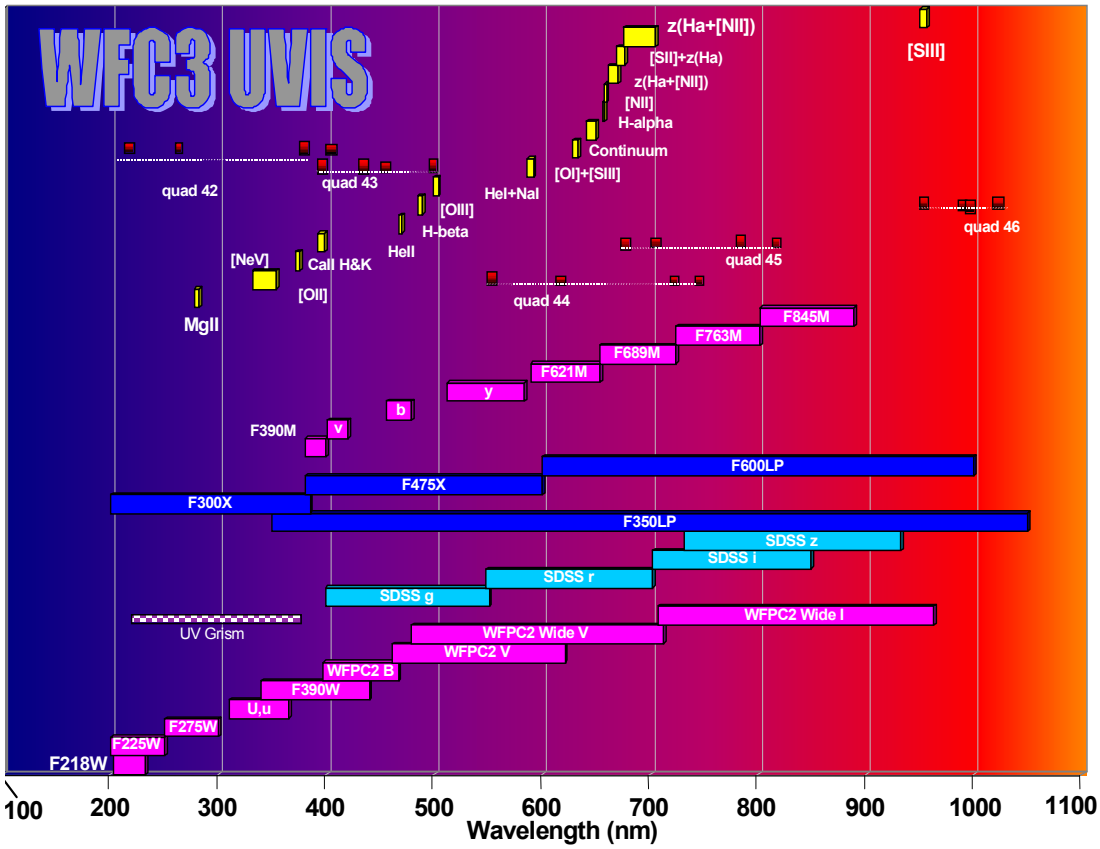

Fig. 8. WFC3 UVIS filter set.

The UV (200-400 nm), a region of the spectrum with relatively low sky brightness, is expected to see frequent use in WFC3 use as ACS and STIS are not optimized for wide field UV imaging. Key projects are likely to include studies of galaxies and star forming regions in the UV, resolved and unresolved stellar populations, interstellar medium emission and dust, and ultra deep surveys (Stiavelli & O'Connell). The increase in grasp in the new replacement UV filters will translate directly into more efficient observing or increased sensitivity for a given exposure time. Aside from the UV and narrow bands, there are also a variety of broad filters on WFC3. Some of these were specified to duplicate filters

used in previous ground and space instruments such as WFPC2 (V [F555W], wide V [F606W] and I [F814W]) and the Sloan Digital Sky Survey (G, r, I, and z), a ground-based optical survey designed to cover more than 25% of the sky. These filter sets will provide a mechanism for continuing and extending previous research done with other instruments. The UVIS filters, in combination with the relatively wide field of view (160"x160") in the UVIS channel and the new detector, are expected to make WFC3 the camera of choice on HST for a wide variety of exciting science projects

IR

As mentioned in the introduction, in contrast to the UVIS filters, none of the IR filters suffered from filter ghosts but two of the IR filters were remade on colored glass, to replace the original fused silica versions that would no longer function as required with the new IR detector. The procurement of these two filters (F110W with bandpass ~0.9-1.4 μm, and F125W with bandpass 1.1-1.4 μm) went smoothly; no problems were found during the characterization tests. Bandpasses of the new versions are nearly identical to the original versions and the new filters satisfy the customary wavefront, focus, and wedge requirements. One of the original IR grisms (g141) removed to correct an installation problem has been remade with a coating to define the red edge at 1.69 μm. Originally, the detector was to provide the red cutoff but ground testing revealed some excess background that could be eliminated with an appropriate filter coating. This element has been procured and characterization testing is in progress.

A single wheel with 18 slots houses the IR filters (one slot is reserved for an opaque blocker). The final IR filter set, illustrated in Figure 9, includes 5 wide, 4 medium, 6 narrow band filters, and two grisms; one of the filters (F093W) has significant blue transmission in order to be used for instrument alignment purposes. The two IR grisms (~0.9-1.15 μm and 1.1-1.7 μm) will serve as complements to the WFC3 UV grism (~220-400 nm) and ACS grism (~600-880 nm).

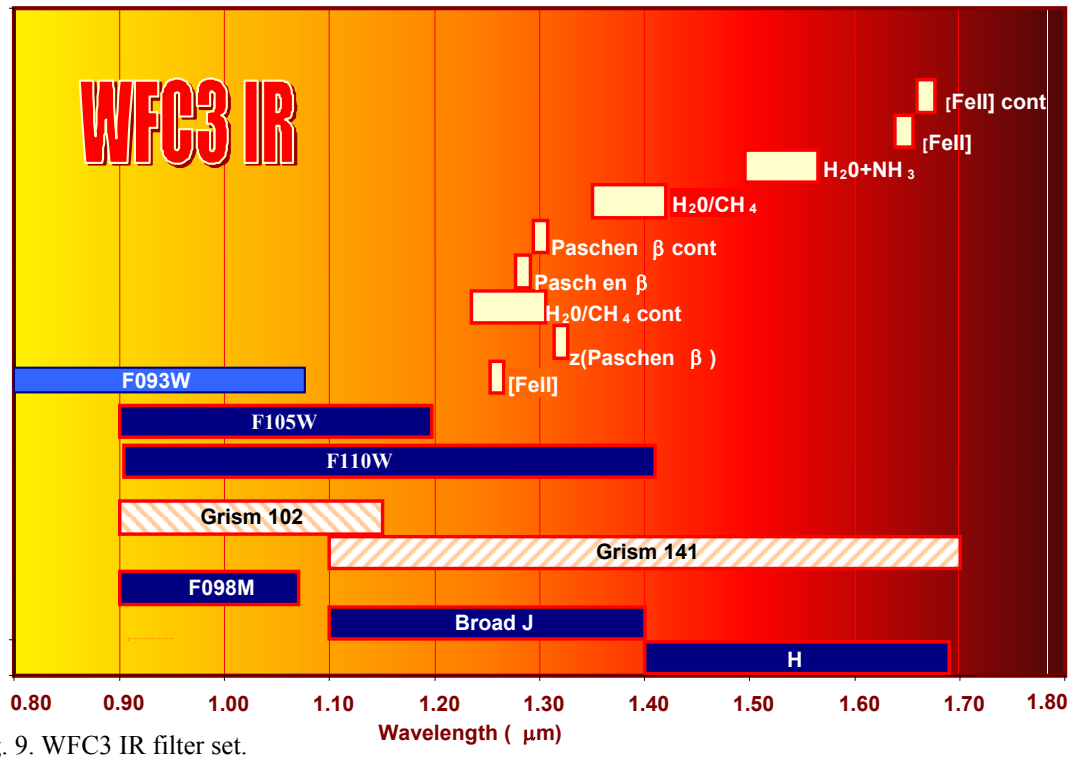

Fig. 9. WFC3 IR filter set.

Scientific studies using the WFC3 IR channel will benefit significantly from its location in low Earth orbit (above the numerous water lines in the Earth's atmosphere and with low OH sky background) as well as its relatively large field of view (123x139", compared to 11"x11" up to 51"x51" for NICMOS, the HST Near Infrared Camera and Multi Object

Spectrometer). A key area for the IR channel is expected to be observations of supernovae, in order to continue research on the problem of dark energy and the accelerating universe (Kimble et.al.). IR wavelengths can also be used to peer through dust-enshrouded targets, view highly red-shifted targets (e.g., those whose UV ~90-121 nm wavelengths have been red-shifted into the IR), observe the atmospheres of planets or detect ices (e.g., with the water, methane, and ammonia filters), search for low mass stars (e.g., with filters like the broad J and H) and image areas in galaxies where dust is absorbing and redistributing energy.

Panchromatic

Finally, there are investigations where the UVIS and IR channels would be most productive when used in combination. For example, galaxy structure and evolution could be explored using a wide spectral range: star forming regions and hot young stars in a galaxy will stand out in the UV, while lower mass, older populations will be detected in the IR. With a better understanding of nearby galaxies, studies could be extended to galaxies at higher redshifts (Stiavelli & O'Connell; Kimble et.al.). Studies of stellar evolution too, would benefit from a panchromatic examination: the UVIS can be used to observe stars of all ages and their associated ejecta, pinning down details such as wind/nebula composition, physical sizes and motions while the IR can be used to penetrate any intervening dust to study the objects within. Closer to home, solar system targets could be studied with both the UVIS and IR channels, for example, to continue meteorological studies of planets started with earlier instruments such as WFPC1, WFPC2, and ACS; the IR can be used to penetrate to the surface of targets otherwise opaque in the UV and visible. Having the best possible filters in place in both channels will help ensure the science will not be limited by hardware but only by the imagination.

REFERENCES

1. "HST WFC3 Capabilities and Science Programs," *WFC3 Science White Paper*, SOC and Science IPT, edited by M. Stiavelli and R. W. O'Connell, 2000.
2. T. M. Brown and O. Lupie, "Filter Ghosts in the WFC3 UVIS Channel," *Instrument Science Report WFC3 2004-04*, April 2004.
3. H. E. Bond and T. M. Brown, "Scientific Impacts of UVIS Channel Filter Ghosts," *Instrument Science Report WFC3 2006-16*, April 2005.
4. N. A. Raouf and J. T. Trauger, "Characterization of UV-visible filters for the Wide Field Camera 3 of the Hubble Space Telescope," *Proc. SPIE*, **4842**, p.301-318, Jan 2003.
5. JPL Specification Document D-18189 Version D, Wide Field Camera-3 (WFC3) Optical Filters, HST Library #TM-031791, Nov 2001.
6. Hubble Space Telescope Wide Field Camera 3 Contract End Item (CEI) Specification, STE-66, HST Library #TM-027550, GSFC, May 2000.
7. Wide Field Camera 3 Infrared Filter Test Plan, HST Library #TM-028642, GSFC, April 2001.
8. Hubble Space Telescope Wide Field Camera 3 Infrared Filters Specification, HST Library #TM-031672, GSFC, July 2003.
9. R. A. Boucarut et al., "Characterization of infrared filters for the Wide Field Camera 3 of Hubble Space Telescope," *Proc. SPIE*, **4441,** p. 142-153, Current Developments in Lens Design and Optical Engineering II, R.E. Fischer, R.B. Johnson, and W.J. Smith, eds., Dec 2001.
10. M. A. Quijada et al., "Images and spectral performance of WFC3 interference filters," *Proc. SPIE*, **6265**, in press (this volume).
11. R. A. Kimble, J. W. MacKenty, R. W. O'Connell, and the WFC3 Team, "Status and performance of the HST Wide Field Camera 3," *Proc. SPIE*, **6265**, in press (this volume).

More WFC3 information is available online

http://www.stsci.edu/hst/wfc3/

http://wfc3.gsfc.nasa.gov